Lai, D., Zhou, X., and Chen, Q. 2017. "Modelling dynamic thermal sensation of human subjects in outdoor environments," *Energy and Buildings*, 149: 16-25.

Modelling Dynamic Thermal Sensation of Human Subjects in Outdoor Environments

Dayi Lai[1], Xiaojie Zhou[2], Qingyan Chen[1,2,*]

[1]School of Mechanical Engineering, Purdue University, West Lafayette, IN 47907, USA

[2]Tianjin Key Lab of Indoor Air Environmental Quality Control, School of Environmental Science and Engineering, Tianjin University, Tianjin 300072, China

*Corresponding author: Qingyan Chen

Phone: +1-765-496-7562, Email: yanchen@purdue.edu

Abstract

Outdoor spaces provide the growing urban population with social, health, environmental, and economic benefits. A thermal comfort model is needed to aid in the design of attractive urban outdoor spaces. In an outdoor environment, a person's thermal comfort changes with the dynamic weather conditions. However, most of the outdoor thermal comfort models in the literature are for steady-state conditions. To develop a dynamic thermal comfort model, this study observed the responses of 26 human subjects from West Lafayette, Indiana, USA, and Tianjin, China, to a wide range of outdoor thermal environments. The study monitored the subjects' skin temperatures, recorded their thermal sensations, and measured several outdoor environmental parameters. Analysis of the test data showed that the thermal load, the mean skin temperature, and the change rate of the mean skin temperature of the subjects tested were the most important parameters affecting their thermal comfort in the outdoor spaces. These three parameters were integrated as predictor variables into a comfort model for predicting the outdoor thermal sensation. The model uses the thermal load to evaluate the thermal environment, and the mean skin temperature, and its change rate to consider dynamic changes in the thermal state of the human body. The validity of the model developed in one region was tested with the use of data obtained from the other region.

Keywords

Thermal comfort model; Outdoor spaces; Thermal load; Human subject test; Dynamic thermal sensation

Highlights

A thermal sensation model was developed for dynamic outdoor thermal environments.

Thermal load, mean skin temperature, and change rate of mean skin temperature are the three predictor variables.

The model was validated for predicting the thermal sensation of human subjects in different regions.

1. Introduction

The global urbanization rate is expected to reach 66.4% in 2050 [1], according to the United Nations. Outdoor spaces in cities provide the growing urban population with social, health, environmental, and economic benefits [2]. One of the goals in urban planning and design is to make outdoor spaces attractive to people and therefore used by them [3]. Researchers have found a strong correlation between activity level and thermal comfort in outdoor spaces [4-8]. Thus, it is important to design urban open spaces with greater thermal comfort in order to attract more citizens.

A thermal comfort model is a useful tool for evaluating the comfort of the microclimate in an outdoor space. A number of studies have used thermal comfort models in the design of comfortable open spaces [9-11]. For instance, Berkovic et al. [10] used the predicted mean vote (PMV) [12] to study the thermal comfort in various courtyards in a hot, arid climate. They concluded that shading was the best way to improve outdoor thermal comfort in that climate. Taleghani et al. [11] employed the physiologically equivalent temperature (PET) [13] to assess the thermal comfort in five urban settings in the Netherlands in the month of June. They found that courtyards had the most comfortable microclimate because they provided the most shade from solar radiation.

While the above studies have demonstrated the usefulness of these models in the design of outdoor spaces, other studies have questioned the models' accuracy. For example, Nikolopoulou et al. [14] and Thorsson et al. [15] found distinct discrepancies between the actual and calculated thermal sensation distributions when using the PMV model. Kantor et al. [16] found that the neutral PET in Hungary differed by as much as 9 K from that in Taiwan [17]. Our earlier study [18] showed substantial differences in the thermal sensation determined by the universal thermal climate index (UTCI) [19] between the Mediterranean climate [20] and the climate in northern China. These discrepancies suggest the need for more accurate thermal comfort models for outdoor spaces.

The development of thermal comfort models for outdoor spaces has followed three different approaches. The first approach uses a regression method to determine outdoor thermal sensation as a function of several climatic parameters (wind speed, solar radiation, air temperature, humidity, etc.) [21]. Although the approach is simple, it is not based on physical principles, and the validity of such a model is limited to the climate regions where the data was obtained [22]. The second approach develops thermal comfort models by correlating thermal sensation with the thermal load of the human body. The most widely used model is the PMV model. However, PMV is based on the data collected during subject tests in controlled indoor chambers, and it is not suitable for outdoor environments [14, 15]. This is because the thermal load calculated by the model can only predict thermal comfort in a steady-state indoor environment, not a dynamic outdoor environment [22, 23]. The third approach is based on physiological responses of human subjects such as skin and core temperatures, PET, UTCI, standard effective temperature (SET*) [24], and outdoor standard effective temperature [25]. Those models use the concept of equivalent temperature, which is the air temperature in an indoor space that produces the same physiological responses as the actual outdoor conditions. Equivalent temperature models do not consider dynamic physiological responses.

Meanwhile, some of the existing thermal comfort models for indoor spaces, such as the local and whole-body thermal sensation model [26] and the dynamic thermal sensation (DTS) model [27], use the dynamic skin and core temperature to predict thermal sensation directly. These models have a solid physiological and physical foundation. Since no existing outdoor thermal comfort model considered the dynamic feature of outdoor thermal environment, this study aims to develop a dynamic outdoor thermal comfort model by using the research method from the development of indoor dynamic models. The present paper reports our effort in developing such model based on this approach. The paper also describes the validation of the model.

2. Research Method

This section describes the procedure for developing a thermal comfort model with a solid physiological and physical foundation. Development of the model required the collection of data by means of human subject tests in outdoor spaces.

2.1.Human subject tests

We performed the human subject tests in Tianjin (TJ), China, and West Lafayette (WL), Indiana, USA. The climatic conditions in the two places allowed us to collect data from a wide variety of thermal environments. In addition, we were able to use data from one region to develop the model, and data from the other region to validate the model. The test in Tianjin were conducted from May 21, 2016, to December 14, 2016, and the tests in West Lafayette from March 6, 2016, to September 25, 2016. The air temperature during the test periods ranged from 0 to 35 ^{o}C. To collect comparable amounts of experimental data at different outdoor air temperatures, we relied on weather forecasts to arrange the test dates. Our tests involved 26 subjects, satisfying the previously reported sample-size requirement of 25 [28]. Each subject participated in the tests between three and five times under different thermal environments. A total of 94 sets of data were obtained, where one set of data consisted of the measured results from one subject in a given test. Table 1 lists the numbers of subjects and data sets according to gender and age for the tests in Tianjin and West Lafayette. Since the Tianjin data was obtained from both male and female subjects with a wide range of ages, we used the Tianjin data to develop the model and the West Lafayette data to perform the validation. We also used the Tianjin data to investigate the outdoor thermal comfort for subjects of different genders and ages.

Table 1. Numbers of subjects and data sets according to gender and age for the tests conducted in Tianjin (TJ) and West Lafayette (WL).

	Location	**Male**	**Female**	**Age < 30**	**Age > 30**	**Total**
Number of subjects	TJ	9	7	10	6	16
	WL	10	0	10	0	10
	Total	19	7	20	6	26
Number of data sets	TJ	30	24	32	22	54
	WL	40	0	40	0	40
	Total	70	24	72	22	94

The test procedures were approved by the Purdue IRB (institutional review board) for human subject experimentation. Before the start of the tests, the subjects were informed of the research objectives and procedures. Each subject signed a consent form before participating in the tests. During the tests, the subjects remained in a neutral indoor chamber for 30 minutes to achieve a stable thermal state. They then walked to an outdoor space and stood there for 60 minutes. Since the walking distance between the indoor and outdoor test spaces is only 50m, we did not consider the walking activity in our study. The air temperature and relative humidity in the indoor chamber was controlled at around 24 ^{o}C and 50%, and the air movement was kept at a minimum. As shown in Figure 1, this investigation monitored the skin temperature of the subjects, recorded their thermal sensation and clothing level, and measured several outdoor environmental parameters. The skin temperature was measured by attaching thermocouples to the head, face, thorax, abdomen, left upper arm, left lower arm, left hand, left upper leg, left lower leg, and left foot of each subject. The thermocouples were connected to portable data loggers. With continuous measurements of skin temperature, the change rates of the skin temperature can be easily obtained. At the same time, we used a questionnaire to collect information about the subjects' clothing and thermal sensation. The clothing information was converted to clothing resistance (CR) with the use of garment insulation values from the ASHRAE Handbook [29]. The subjects recorded their thermal sensation vote (TSV) according to the ASHRAE [29] seven-point scale, where -3 = cold, -2 = cool, -1 = slightly cool, 0 = neutral, 1 = slightly warm, 2 = warm, and 3 = hot. We allowed the subjects to rate their thermal sensation continuously along this scale. During the one-hour outdoor exposure, the subjects recorded their thermal sensation every five minutes. Thus, 12 thermal sensation values were obtained for each subject during a given outdoor test. To reduce the uncertainty caused by solar radiation in the outdoor spaces, the subjects stood with their backs to the sun. The recorded outdoor thermal environmental parameters included air temperature, T_a; relative humidity, RH; global radiation, G; and wind speed, V_a. In Tianjin, we used a portable weather station to measure these parameters. In West Lafayette, the T_a, RH, and G were monitored on the rooftop of a surrounding building. The V_a was recorded by a handheld anemometer. Table 2 provides information about the instruments used in the subject tests.

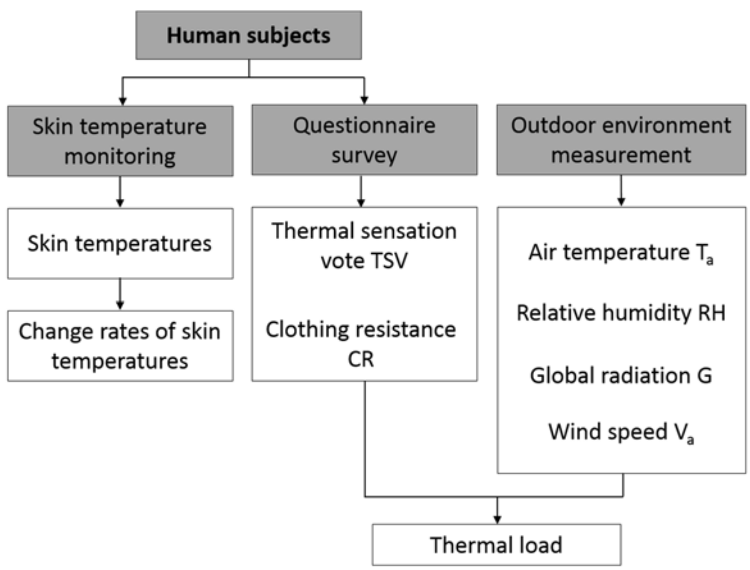

Figure 1. Parameters obtained in the outdoor human subject tests.

Table 2. Sensors used to measure thermal environmental parameters and skin temperature.

Parameter	Sensor	Range	Accuracy	Interval
T_a	S-THB-M002	-40 to 75 °C	±0.2 K at 20 °C	1 min.
RH	S-THB-M002	0 to 100%	±3%	1 min.
V_a, WL	WM4	0.35 to 40 m/s	±3%	5 min.
G, WL	SPN1	0 to > 2000 W/m^2	±5% ± 10 W/m^2	5 min.

V_a, TJ	S-WSET-A	0–45 m/s	±1.1 m/s	1 min.
G, TJ	S-LIB-M003	0-1280 W/m^2	±10 W/m^2 or ±5%	1 min.
T_{sk}	TT-K-30-SLE	0 to 350 ^{o}C	±1.1 ^{o}C or ±0.4%	1 sec.

The thermal load (TL) of the subjects could not be directly measured during the tests. This study calculated the thermal load by using the T_a, RH, G, V_a, CR, and metabolic heat production rate (MET). According to the ASHRAE Handbook [29], the metabolic rate of a standing person can be estimated at 70 W/m^2. The thermal load per unit of skin area is defined as the rate of heat gain or loss by an individual when his or her skin temperature is maintained at a neutral level and sweating is kept to a minimum:

$$TL = (M - W + R_S) - (C + R_L + E_{sk} + C_{res} + E_{res}) \quad (1)$$

where M is the rate of metabolic heat production (W/m^2), W the rate of mechanical work (W/m^2), R_S the rate of short-wave radiative heat gain (W/m^2), C the rate of convective heat loss (W/m^2), R_L the rate of long-wave radiative heat loss (W/m^2), E_{sk} the rate of evaporative heat loss from the skin (W/m^2), and C_{res} and E_{res} the rates of convective and evaporative heat loss, respectively, from respiration (W/m^2). The calculation of each term is based on the human heat transfer model developed earlier by the authors [30].

2.2.General procedure for development of the model

The data obtained from the human subject tests was used to develop the outdoor thermal sensation model. As shown in Figure 2, this investigation assumed that thermal sensation is determined by three groups of parameters: the heat transfer parameters (T_a, RH, G, V_a, CR, MET, and TL); the skin temperatures T_{sk} at different body segments and the mean skin temperature $T_{sk,m}$; and the change rates of the skin temperatures, dT_{sk}/dt and $dT_{sk,m}/dt$. We obtained the mean skin temperature $T_{sk,m}$ by weighting the skin temperatures at different body parts. When the mean skin temperature has been determined, the change rate of mean skin temperature can be easily calculated.

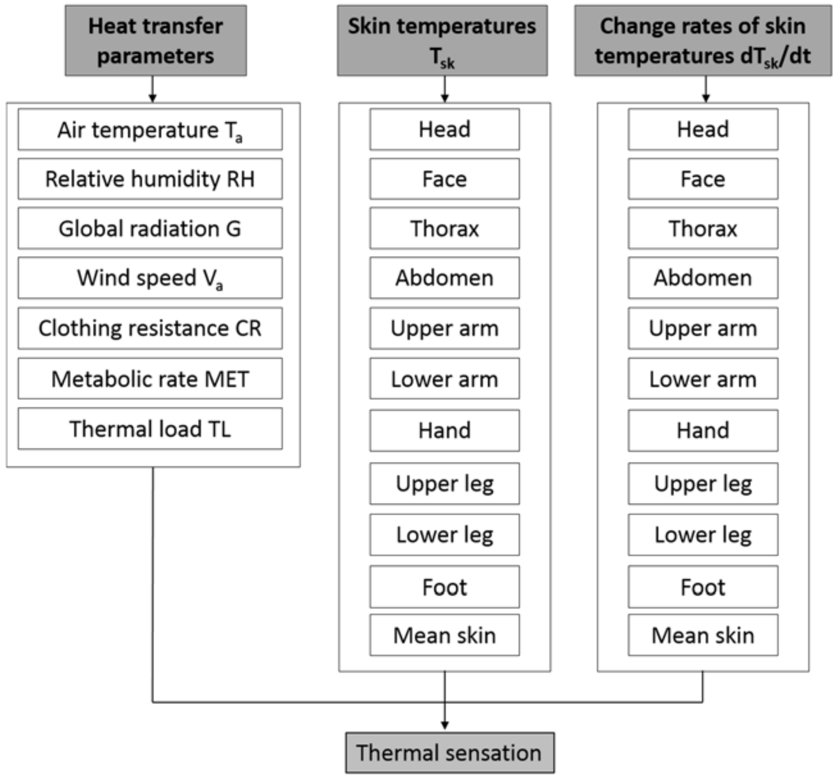

Figure 2. Three groups of parameters related to thermal sensation.

The first step in development of the model was to select the most significant parameters from the three groups as the predictor variables. The model should involve the smallest number of variables that can adequately represent the influences on outdoor thermal sensation. To select the predictor variables, this investigation used the Spearman correlation coefficient [31], r_s, to study the correlations between the influencing parameters and thermal sensation. The coefficient is a non-parametric measure of the strength and direction of association between two variables. The value of r_s ranges between -1 and 1, and a higher absolute value indicates a stronger association. The statistical software program R [32] was used to determine r_s. This investigation selected the parameters with high r_s from the three groups.

After the most significant parameters had been selected, the next step was to determine the function form of the model. According to our observation, the logistic function [26] could represent the thermal sensation and the predictor variables. The general form of the logistic function can be written as:

$$y = A\left(1 - \frac{2}{1 + \exp\left(\sum_i B_i \cdot x_i\right)}\right) \tag{2}$$

where A is the limit coefficient and B is the slope coefficient. As shown in Figure 3, the relationship between x and y is linear when the value of x is small. As x increases or decreases, the value of y reaches the upper limit of A or the lower limit of -A. Because in our study, the value of thermal sensation never exceeded the upper limit of 3 or lower limit of -3. This study selected the logistic function as a candidate because it can mimic the limits of thermal sensation. Furthermore, we can see that a function with a larger B has a greater slope. For this application, y is thermal sensation and A represents the limits of thermal sensation.

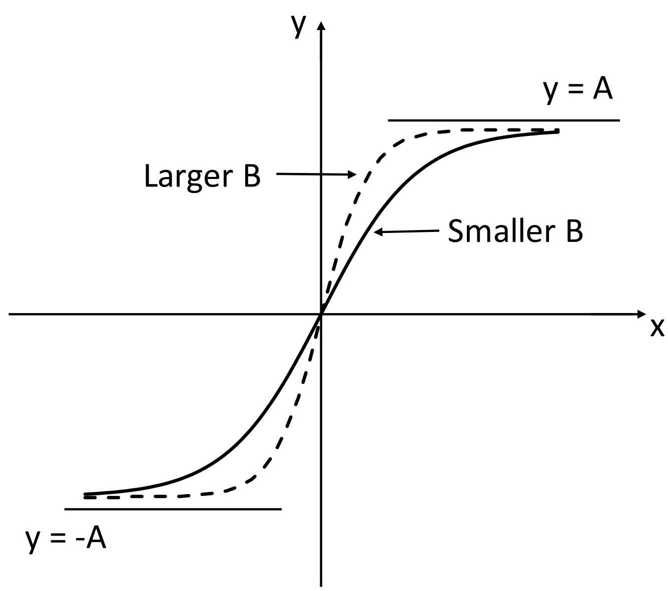

Figure 3. Illustration of the logistic function.

3. Results

This section describes our development of the outdoor thermal sensation model and validation of the model. First, we showed the measured outdoor thermal environmental parameters. Next, we selected the predictor variables on the basis of the correlation analysis described above. We then determined and validated the mathematical expression of the model.

3.1.Outdoor thermal environment

Table 3 summarizes the measured mean, standard deviation, maximum, and minimum of air temperature T_a, relative humidity RH, wind speed V_a, and global radiation G during the subject tests in West Lafayette and Tianjin. The air temperature ranged from -0.1 to 35.0 ^{o}C. The measured wind speed ranged from 0.2 to 2.9 m/s. In Tianjin, the wind speed was lower than that in West Lafayette. The climatic conditions during the tests have a wide range and correspond to the typical outdoor thermal environment in the two places.

Table 3. The measured mean, standard deviation, maximum, and minimum of air temperature T_a, relative humidity *RH*, wind speed V_a, and global radiation *G* in West Lafayette and Tianjin during the subject tests.

		T_a (ºC)	***RH*** **(%)**	V_a (m/s)	G (W/m^2)
WL	Average	15.7	60.0	1.5	437
	Stdev.	10.4	14.1	0.9	262
	Max.	33.8	86.9	0.4	132
	Min.	-1.0	38.4	2.9	960
TJ	Average	18.2	47.8	0.7	341
	Stdev.	10.6	21.5	0.4	274
	Max.	35.0	89.3	2.0	19.0
	Min.	1.9	21.0	0.2	904

3.2.Selection of predictor variables

Table 4 shows the values of the Spearman correlation coefficient, r_s, for the correlations between the heat transfer parameters and thermal sensation. The r_s values for clothing resistance, relative humidity, and wind speed were negative, which indicates that increases in these parameters were associated with a decrease in thermal sensation. The negative association between clothing resistance and thermal sensation is counter-intuitive at first glance, since people feel warmer when they are wearing more clothing. However, in an outdoor space, when the air temperature is lower, people feel colder and wear more clothing to keep warm. Thus, the inverse association between CR and T_a is the reason for the negative r_s of CR. The same is true for the negative r_s of RH, since a high outdoor air temperature was often associated with a low relative humidity in our tests. The thermal load had the highest r_s, 0.85, among the heat transfer parameters. Thermal load is an artificial parameter that indicates the imbalance of heat in a human body with hypothetical neutral skin temperature and sweat secretion. If this neutral human body has a thermal load, it means that heat exchange exists between the environment and the body. As a result, the body will deviate from the neutral state. The larger the thermal load, the greater the deviation. Because of the high level of correlation between thermal load and thermal sensation, we selected TL as a predictor variable in the outdoor thermal sensation model. Although the r_s for the correlation between T_a and thermal sensation is 0.83, we did not include it in our model. This is because the r_s for the correlation between TL and T_a is as high as 0.86. The high correlation between two predictor variables can cause multicollinearity [31] problem, which will make the coefficient estimate unstable and difficult to interpret.

Table 4. Spearman correlation coefficient, r_s, for the correlations between heat transfer parameters and thermal sensation.

Parameters	TL	T_a	CR	G	RH	V_a
r_s	0.85	0.83	-0.74	0.41	-0.28	-0.19

Although thermal load can indicate the general direction and magnitude of thermal sensation, it does not take into account the dynamic influence of weather conditions on the body's thermal state. Skin temperature is a good indication of this influence because the thermoreceptors in the skin sense the skin temperature and send a signal to the brain, which interprets the signal as thermal sensation in real time [26]. Table 5 shows the values of r_s between the thermal sensation and the skin temperatures, including the mean skin temperature $T_{sk,m}$ and the skin temperatures at different body parts. The face, head and hand, which were exposed to the outdoor environment, had higher r_s than the thorax and abdomen, which were not exposed. Because of high thermal inertia and clothing insulation, the responses of the non-exposed body parts to the dynamic outdoor thermal environment were not as fast as the responses of the exposed body parts. The mean skin temperature had the highest r_s among all the skin temperatures because it integrated the thermoreceptors' signals from all over the body. As a result, this investigation selected $T_{sk,m}$ as another predictor variable in the model.

Table 5. Spearman correlation coefficient, r_s, for the correlations between skin temperatures and thermal sensation.

Skin temperatures	Mean skin	Face	Head	Hand	Lower leg	Upper leg
r_s	0.85	0.84	0.81	0.79	0.78	0.77
Skin temperatures	**Upper arm**	**Feet**	**Lower arm**	**Thorax**	**Abdomen**	
r_s	0.68	0.63	0.50	0.24	0.14	

Weather conditions also have a dynamic effect on the change rate of skin temperature. The thermoreceptors in the skin respond to changing skin temperature at a higher stimulating rate than to steady skin temperature [33]. For example, a person feels colder when his or her skin temperature is decreasing than when the skin temperature is constant. Table 6 lists the r_s values for the correlations between the change rates of skin temperatures and the thermal sensation. Although the r_s was not as high as that for thermal load and skin temperatures, the value for the change rate of mean skin temperature show moderate correlations. Because the change rate of $T_{sk,m}$ had the highest r_s among the values shown in the table, we selected it as the third predictor variable in the model.

Table 6. Spearman correlation coefficient, r_s, for correlations between change rates of the skin temperatures and thermal sensation.

dT_{sk}/dt	**Mean skin**	**Feet**	**Upper leg**	**Hand**	**Upper arm**	**Lower leg**
r_s	0.51	0.47	0.44	0.43	0.38	0.36
dT_{sk}/dt	**Face**	**Lower arm**	**Head**	**Abdomen**	**Thorax**	
r_s	0.33	0.32	0.13	0.10	0.08	

Thus, on the basis of the above correlation analysis, this study selected thermal load (TL), mean skin temperature ($T_{sk,m}$), and the change rate of mean skin temperature ($dT_{sk,m}/dt$) as the three predictor variables for determining an outdoor thermal sensation, TS, expressed as:

$$TS = f(TL, T_{sk,m}, \frac{dT_{sk,m}}{dt}) \quad (3)$$

3.3.Mathematical expression of the outdoor thermal sensation model

To determine the mathematical expression for the outdoor thermal sensation model, we examined scatter plots of the thermal load, mean skin temperature, and change rate of mean skin temperature with respect to thermal sensation. As shown in Figures 4(a), 4(b), and 4(c), the relationships between the three variables and TS were roughly linear. However, because of the nature of thermal sensation, its absolute value never exceeded the limits of 3 and -3, and therefore the actual relationship is not linear. Next, we examined the average values of the predictor variables. The relationships between mean thermal sensation and the mean TL, $T_{sk,m}$, and $dT_{sk,m}/dt$, as shown in Figures 4(d), 4(e), and 4(f), respectively, resemble the shape of the logistic function (see Figure 3). Thus, the logistic function would give a good fit to the data.

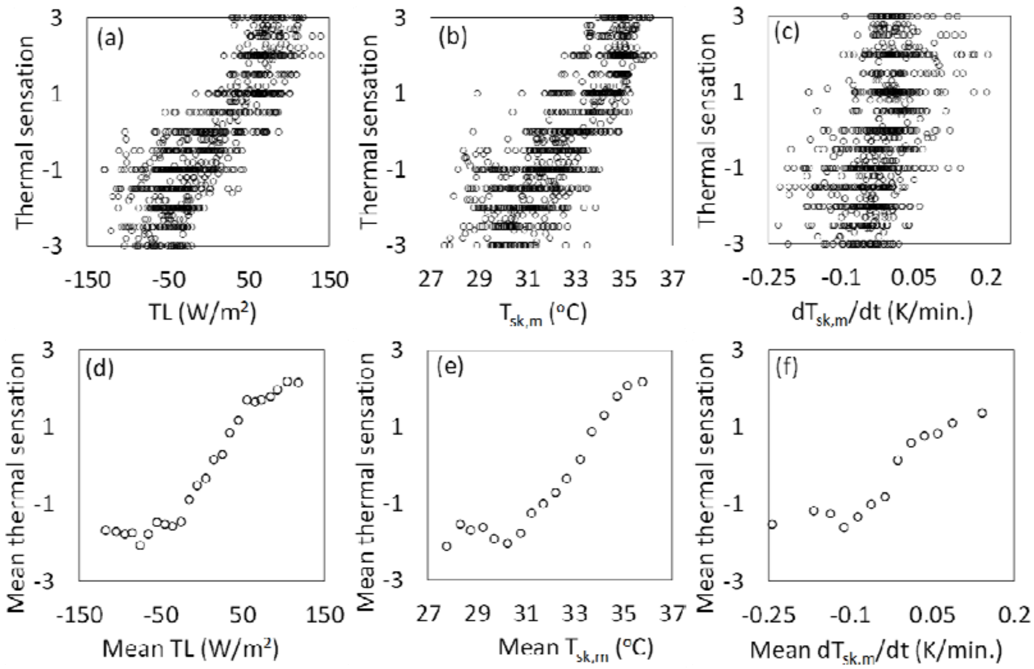

Figure 4. Test data for the predictor variables: (a) TS vs. TL, (b) TS vs. $T_{sk,m}$, (c) TS vs. $dT_{sk,m}/dt$, (d) mean TS vs. mean TL, (e) mean TS vs. mean $T_{sk,m}$ (f) mean TS vs. mean $dT_{sk,m}/dt$.

Because the thermal sensation limits are 3 and -3, the coefficient A in Eq. (2) is 3. The model becomes:

$$TS = 3\left(1 - \frac{2}{1 + \exp\left(B_1 \times TL + B_2 \times \Delta T_{sk,m} + B_3 \times \frac{dT_{sk,m}}{dt}\right)}\right) \quad (4)$$

where $T_{sk,m}$ is replaced by $\Delta T_{sk,m}$, the difference between the actual and neutral $T_{sk,m}$. The neutral $T_{sk,m}$ was 32.73 °C, which was obtained by averaging the $T_{sk,m}$ when the subjects voted for neutral in the outdoors. The TL, $\Delta T_{sk,m}$, and $dT_{sk,m}/dt$ act as the stimuli for outdoor thermal sensation. The TS is neutral if these stimuli are absent. When the stimuli are positive or negative, the resulting TS is on the warm or cold side. The B_1, B_2, and B_3 are coefficients for TL, $\Delta T_{sk,m}$, and $dT_{sk,m}/dt$, respectively. The data plotted in Figures 4(d), 4(e), and 4(f) reveals asymmetries in warm and cold sensation. For example, in Figure 4(d), the thermal sensation approaches the cold limit faster than the warm limit. Table 7 lists the coefficients that reflect the asymmetry for cold and warm sensation. The R^2 value of the model is 0.811, which indicates a very good fit of the model to the data.

Table 7. Model coefficients B_1, B_2, and B_3.

Coefficient	**B_1 (m^2/W)**	**B_2 (1/K)**	**B_3 (min./K)**
Cold (TL < 0)	0.0124	0.40	0.80
Warm (TL > 0)	0.0102	0.35	0.35

Figure 5 is a graphical interpretation of the model. Larger stimuli result in a greater deviation from zero (neutral). If the stimuli have very large positive values, the right term in the parentheses in Eq. (4) vanishes and the TS is 3. If the stimuli have very large negative values, the exponential of the linear combination in the equation is zero and the TS is -3. As shown in Figure 5, when $T_{sk,m}$ is at its neutral level ($\Delta T_{sk,m}$ = 0 K) and the mean skin temperature is stable ($dT_{sk,m}/dt$ = 0 K/min.), the model is a function only of thermal load, and TS is represented by the solid line in the figure. Because of fluctuating wind speed and the broad ranges of the outdoor thermal environmental parameters, the skin temperature usually deviates from the neutral level ($\Delta T_{sk,m} \neq 0$ K) and is constantly changing ($dT_{sk,m}/dt$ $\neq 0$ K/min.). When the $T_{sk,m}$ changes, the thermal sensation changes correspondingly. This contributes to the transient aspect of the model. Figure 5 shows that when $T_{sk,m}$ deviates from the neutral level by 3 K, TS changes by an amount ranging from 0.6 to 1.6. The figure also demonstrates that the effect of the change rate of $T_{sk,m}$ is minor. A rate of 0.2 K/minute changes the TS by an amount ranging from 0.1 to 0.2.

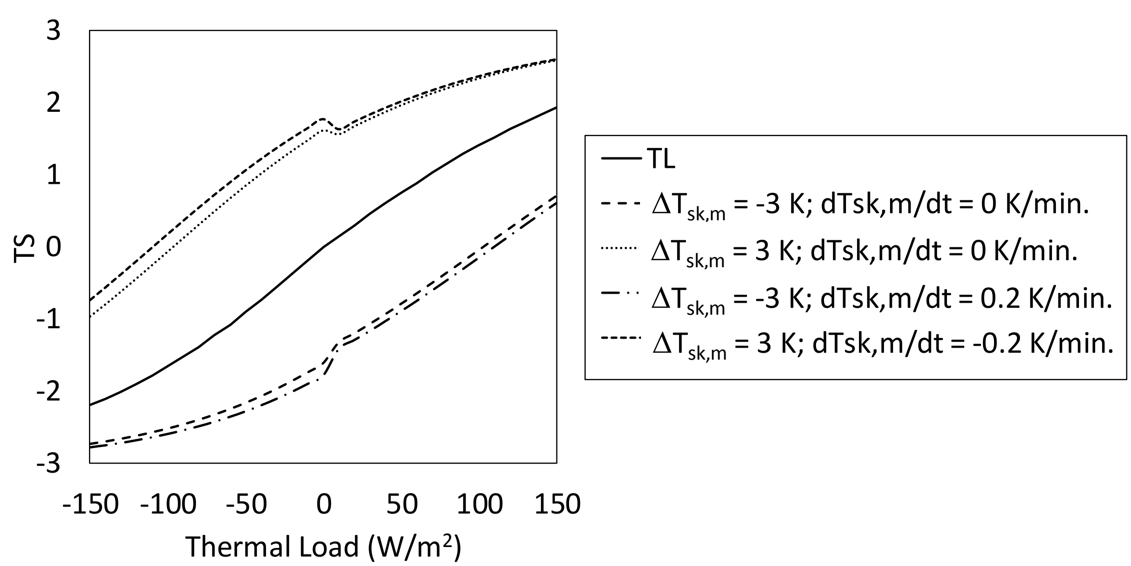

Figure 5. Graphical representation of the outdoor thermal sensation model for thermal load and mean skin temperature change.

Since the impact of $dT_{sk,m}/dt$ on thermal sensation is small, we only conducted sensitivity analyses for $\Delta T_{sk,m}$ and TL, as shown in Figure 6 and Figure 7. From Figure 6, 1 K change in $\Delta T_{sk,m}$ could lead to 0.1 to 0.6 of change in thermal sensation. The impact is highest when the TL = 0 W/m^2. As the absolute value of TL increases, because of the decreasing slopes of the logistic function, the influence from $\Delta T_{sk,m.}$ decreases. Similarly, From Figure 7, we can see that a 50 W/m^2 change in TL could lead to 0.2 to 0.9 of change in thermal sensation. The highest impact is at when the $T_{sk,m}$ is at its neutral level. As the $T_{sk,m}$ deviates from the neutral value, the impact of TL decreases.

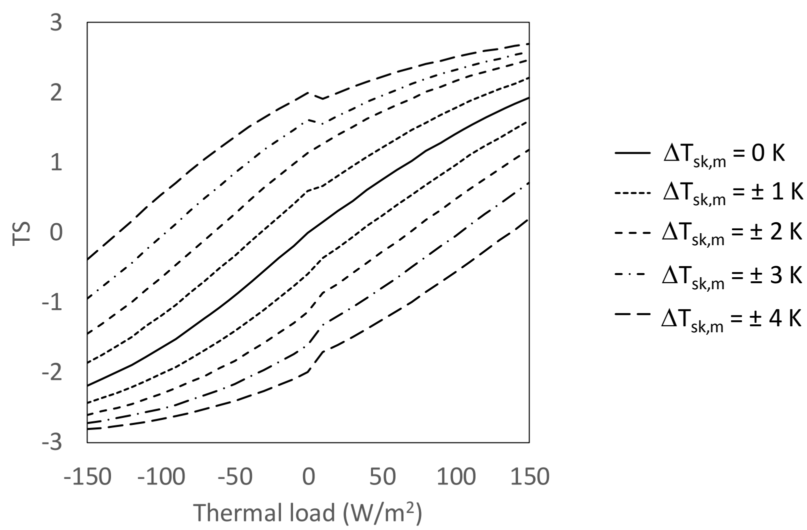

Figure 6. Sensitivity analysis for $\Delta T_{sk,m}$ when dTsk,m/dt = 0.

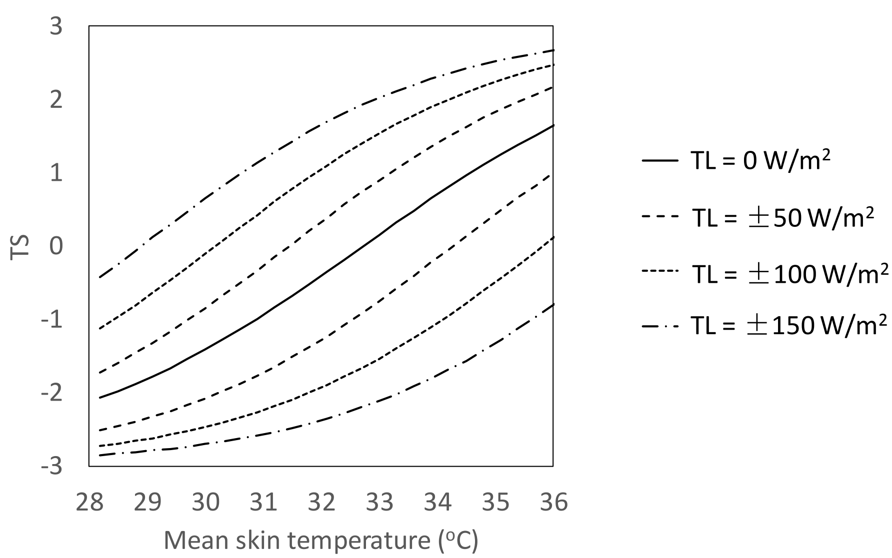

Figure 7. Sensitivity analysis for TL when dTsk,m/dt = 0.

3.4.Validation of the model

Our development of the model above was based on data from Tianjin. We then used the model to predict subjects' thermal sensations in West Lafayette and compared them with the actual data in order to validate the model. This investigation first compared the actual and predicted mean thermal sensation. The mean thermal sensation was obtained by averaging the thermal sensation values within a certain range of TL and $T_{sk,m}$. The intervals of TL and $T_{sk,m}$ used in the averaging process were 20 W/m^2 and 1 K, respectively. For example, the thermal sensation values TL between 20 to 40 W/m^2 and $T_{sk,m}$ between 33 to 34 ^oC were grouped into one case. The TL, $T_{sk,m}$, and $dT_{sk,m}/dt$ within that case were averaged to calculate the predicted mean thermal sensation, which was then compared with the actual mean thermal sensation. Only cases with more than five thermal sensation values were used. Figure 8 compares the 31 eligible cases. The error bars indicate the standard deviations of the actual thermal sensations. Although the model slightly overpredicted the mean thermal sensation, the predictions were still within the ranges of the error bars. The average difference between the actual and predicted thermal sensation was 0.40, while the standard deviation of that difference was 0.27. In light of the wide ranges and frequent fluctuations of thermal environmental parameters in outdoor spaces, the performance of the model in predicting the outdoor thermal sensation is acceptable.

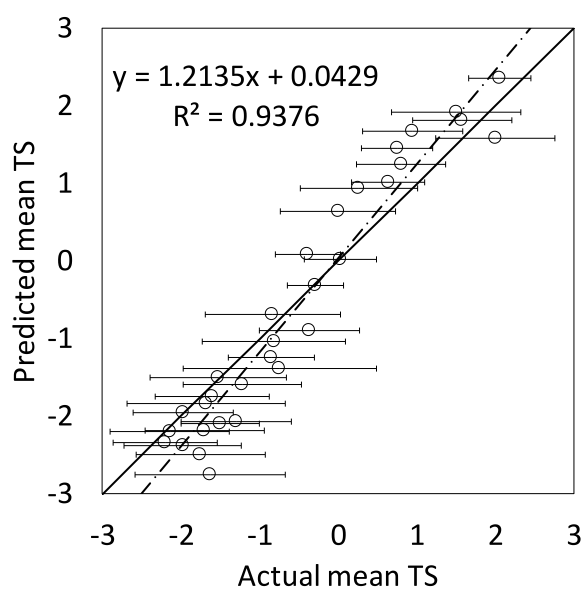

Figure 8. Comparison between the actual and predicted mean thermal sensation.

Please note that the above validation used the mean thermal sensation. It is also worthwhile to evaluate the model's performance in predicting individual thermal sensations. Figure 9 compares the individual actual thermal sensations in West Lafayette with the predicted values. The results show that in 79.6% of the cases, there was a difference of less than one between the predicted and measured thermal sensation. The R^2 between the actual and predicted values in Figure 9 was 0.766, which was only 0.045 less than the model R^2 of 0.811. The closeness of these R^2 values indicates that the Tianjin model did not lose accuracy when applied to West Lafayette. Thus, our model has been validated.

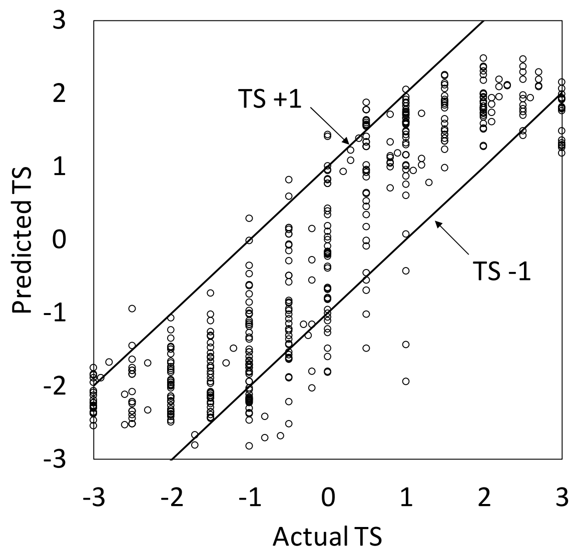

Figure 9. Comparison between the predicted and actual individual thermal sensation. "TS +1" and "TS -1" are the lines where predictions are one unit higher or lower than the actual value.

4. Discussion

4.1 Comparison with the PMV model

The predicted mean vote model employs thermal load to predict thermal sensation in an indoor environment. This study collected thermal load and thermal sensation data in an outdoor environment, and it was worthwhile to compare this data with the results predicted by the PMV model. Since the outdoor data was collected from human subjects who were in a standing position, we assumed a metabolic rate of 70 W/m^2 when calculating the PMV. It can be seen in Figure 10 that the thermal sensation predicted by the PMV model is almost two times the outdoor value. This finding is in accordance with previous results from Nikolopoulou et al. [14], Thorsson et al. [15], and Lai et al. [18]. In their field studies, the PMV model over-predicted the outdoor thermal sensation considerably.

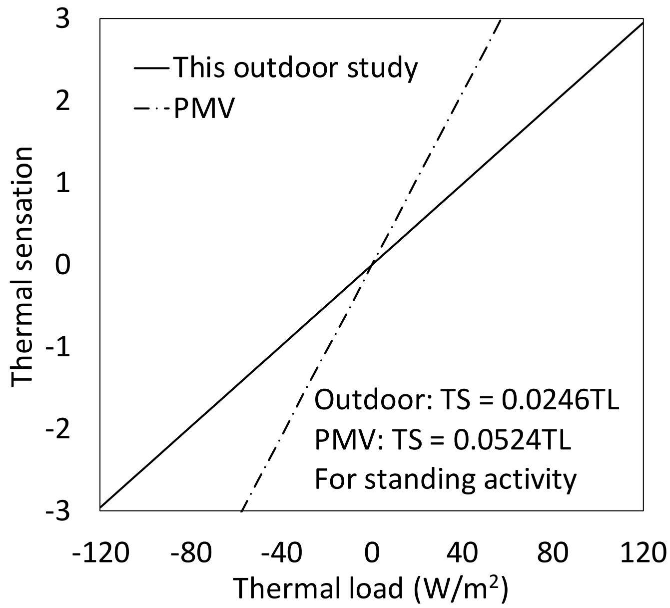

Figure 10. Relationship between thermal load and thermal sensation in the outdoor study and as predicted by the PMV model.

4.2 Alliesthesia

The scatter plot in Figure 4(b) shows that a wide range of skin temperatures can lead to the same thermal sensation. For instance, when the thermal sensation was neutral, $T_{sk,m}$ ranged from 29 to 35 °C. One reason for the variation is the “alliesthesia” effect, which reflects the change in a person’s feeling when the deviation from a certain state is ameliorated [34]. Figure 11 provides two examples of “alliesthesia” from our subject tests. In Figure 11(a), the $T_{sk,m}$ of one subject in cold outdoor condition decreased for the first half hour, and his thermal sensation decreased accordingly, to -3. During the second half hour, the $T_{sk,m}$ of the subject increased slightly. This increase changed his thermal sensation gradually from -3 to 1. At the end of the test, his thermal sensation was approximately neutral, while his $T_{sk,m}$ was only about 29 °C. Figure 11(b) reveals a trend in the opposite direction in hot conditions. At the end of the test, the thermal sensation of the subject was around neutral, and his $T_{sk,m}$ was 34.6 °C. These two examples show that when the thermal state of a person’s body deviates considerably from the neutral state, a slight reversal in the trend of mean skin temperature can change the thermal sensation significantly. In an outdoor environment, alliesthesia is common because the body often deviates from the neutral state, and the changing outdoor thermal environment frequently remedies the deviation.

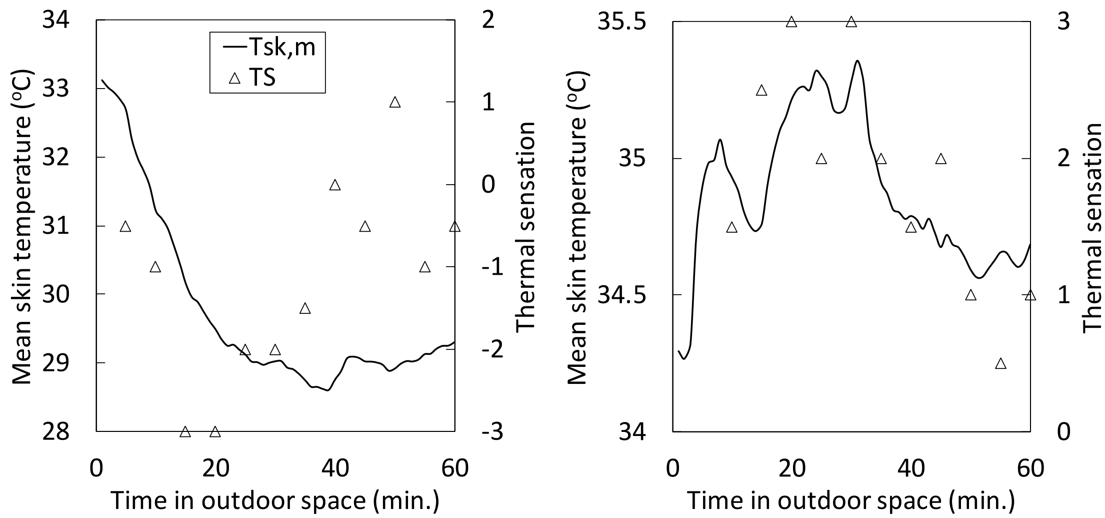

(a) (b)

Figure 11. Variation in TS with $T_{sk,m}$ (a) in a cold outdoor condition and (b) in a hot outdoor condition.

4.3 Gender and age difference

This investigation also used the Tianjin data to study the impact of gender on thermal sensation, and we used the physiologically equivalent temperature (PET) to include various changes in outdoor climate conditions. In order to establish the relationship between the PET and TS, this study calculated the mean TS for every 1 K PET interval. Figure 12 shows the relationship between PET and mean TS for male and female subjects. The similar linear regression lines indicate that the gender difference was negligible. In cold conditions, the average clothing value from the female subjects was 0.18 clo higher than that of the male subjects. The metabolic rate of females is known to be around five to ten percent lower than that of males [35], and the females in our study might have worn more clothing to compensate for their lower metabolism. In other test conditions, we found that there was no difference in clothing value between male and female subjects.

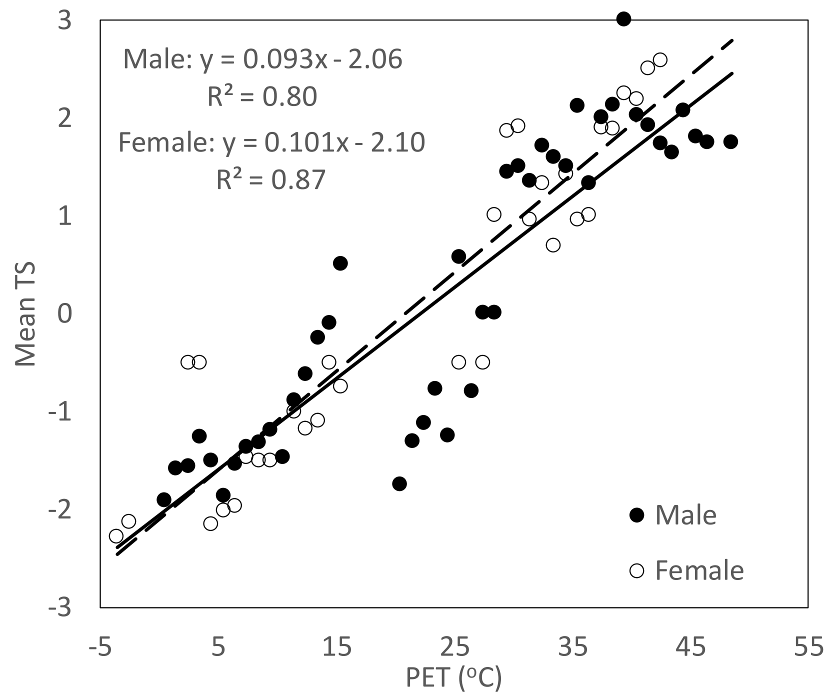

Figure 12. Relationships between PET and mean TS for male and female subjects.

Figure 13 compares the TS for subjects who were under and over 30 years of age. The results show that there was little difference between the two age groups. Note that for the tests conducted in cold conditions, the subjects aged above 30 wore 0.36 clo more clothing, on average, than the younger subjects. The human metabolic rate decreases as people become older [36], and in our study the older subjects compensated for their lower metabolism by wearing more clothing.

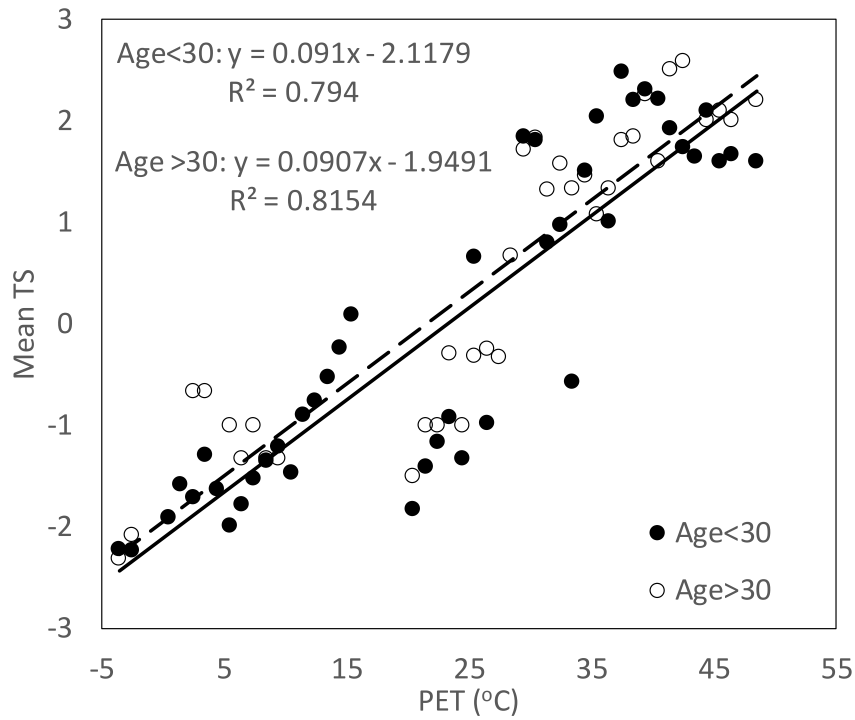

Figure 13. Relationships between PET and mean TS for subjects who were under and over 30 years of age

4.4 Limitations of this study

Outdoor activities typically include sitting, standing, walking, and various levels of exercise, whereas our human subject tests considered only standing activities. However, this study has provided a procedure for developing an outdoor thermal sensation model. In future studies, the model can be further developed for all kinds of outdoor activities. The metabolic rate in our study for a standing person is assumed to be 70 W/m^2. However, the actual metabolic rate may deviate from 70 W/m^2. This caused uncertainty in the thermal load calculation.

The core temperature of the human body is an important physiological parameter that influences thermal comfort. However, the large inter- and intra-personal variability of the core temperature [26] and the difficulties in measuring it in open outdoor conditions prevented us from studying its impact in this study.

Note that the weather conditions in Tianjin and West Lafayette were similar. According to the Koppen climate classification system [37], both cities are in “hot summer continental” climates. It is necessary to validate our model for use in other climates.

5. Conclusions

This study developed a dynamic outdoor thermal sensation model by conducting tests on 26 human subjects in West Lafayette, Indiana, USA, and Tianjin, China. The study led to the following conclusions:

The investigation monitored the skin temperature of the subjects, recorded their thermal sensation and clothing level, and measured several outdoor environmental parameters. This study found that the thermal load, the mean skin temperature, and the change rate of the mean skin temperature were the three most important parameters influencing thermal sensation. The thermal load represents the impact of the thermal environment on the thermal sensation, while mean skin temperature and its change rate are indicators of the dynamic influences of the environment on the body's thermal state.

By analyzing the data, this investigation found that the thermal comfort model for outdoor environments can be described by a logistic function. With the use of the thermal load, the difference between the actual and neutral skin temperature, and the change rate of the mean skin temperature, this investigation developed a thermal comfort model for predicting the outdoor thermal sensation.

This study found that the thermal comfort model developed from the test data from Tianjin can reasonably predict the thermal sensation of subjects in West Lafayette. There was little difference in outdoor thermal sensation for subjects of different gender and age. The model was developed with the use of data from subject tests in hot summer continental climates, and its validity for other climate types needs to be verified.

Acknowledgement

This research was partially supported by the national key project of the Ministry of Science and Technology, China, on "Green Buildings and Building Industrialization" through Grant No. 2016YFC0700500 and the China Scholarship Council (CSC).

References

[1] United Nations. World Urbanization Prospects. <https://esa.un.org/unpd/wup/publications/files/wup2014-highlights.Pdf>, 2014.

[2] H. Woolley, Urban Open Spaces, Taylor and Francis, Abingdon, 2003.

[3] J. Gehl, L. Gemzøe, Public Spaces, Public Life, Danish Architectural Press and the Royal Danish Academy of Fine Arts, School of Architecture Publishers, Copenhagen, 2004.

[4] T.P. Lin, K.T. Tsai, C.C. Liao, Y.C. Huang, Effects of thermal comfort and adaptation on park attendance regarding different shading levels and activity types, Building and Environment 59 (2013) 599-611.

[5] J. Zacharias, T. Stathopoulos, H. Wu, Microclimate and downtown open space activity, Environment and Behavior 33 (2001) 296–315.

[6] M. Nikolopoulou, S. Lykoudis, Thermal comfort in outdoor urban spaces: Analysis across different European countries, Building and Environment 41(11) (2006) 1455-1470.

[7] L. Katzschner, Behavior of people in open spaces in dependence of thermal comfort conditions, PLEA 2006 – The 23rd conference on passive and low energy architecture, Geneva, Switzerland, 2006.

[8] S. Thorsson, T. Honjo, F. Lindberg, I. Eliasson, E.M. Lim, Thermal comfort and outdoor activity in Japanese urban public places, Environment and Behavior 39(5) (2007) 660-684.

[9] H. Chen, R. Ooka, K. Harayama, S. Kato, X. Li, Study on outdoor thermal environment of apartment block in Shenzhen, China, with coupled simulation of convection, radiation and conduction, Energy and Buildings 36(12) (2004) 1247-1258.

[10] S. Berkovic, A. Yezioro, A. Bitan, Study of thermal comfort in courtyards in a hot arid climate, Solar Energy 86 (2012) 1173-1186.

[11] M. Taleghani, L. Kleerekoper, M. Tenpierik, A. van den Dobbelsteen, Outdoor thermal comfort within five different urban forms in the Netherlands, Building and Environment 83 (2015) 65-78.

[12] P.O. Fanger, Thermal Comfort, McGraw Hill, New York, 1972.

[13] P. Höppe, Heat balance modelling, Experientia 49 (1993) 741-746.

[14] M. Nikolopoulou, N. Baker, K. Steemers, Thermal comfort in outdoor urban spaces: Understanding the human parameter, Solar Energy 70(3) (2001) 227-235.

[15] S. Thorsson, M. Lindqvist, S. Lindqvist, Thermal bioclimatic conditions and patterns of behavior in an urban park in Göteborg, Sweden, International Journal of Biometeorology 48(3) (2004) 149-156.

[16] N. Kántor, J. Unger, Á. Gulyás, Subjective estimations of thermal environment in recreational urban spaces—Part 2: International comparison, International Journal of Biometeorology 56 (2012) 1089-1101.

[17] T.P. Lin, Thermal perception, adaptation and attendance in a public square in hot and humid regions, Building and Environment 44 (2009) 2017-2026.

[18] D. Lai, D. Guo, Y. Hou, C. Lin, Q. Chen, Studies of outdoor thermal comfort in northern China, Building and Environment 77 (2014): 110-118.

[19] P. Bröde, D. Fiala, K. Błażejczyk, I. Holmér, G. Jendritzky, B. Kampmann, B. Tinz, G. Havenith, Deriving the operational procedure for the Universal Thermal Climate Index (UTCI), International Journal of Biometeorology 56(3) (2012) 481-494.

[20] K. Pantavou, G. Theoharatos, M. Santamouris, D. Asimakopoulos, Outdoor thermal sensation of pedestrians in a Mediterranean climate and a comparison with UTCI, Building and Environment 66 (2013) 82-95.

[21] D. Lai, C. Zhou, J. Huang, Y. Jiang, Z. Long, Q. Chen, Outdoor space quality: A field study in an urban residential community in central China, Energy and Buildings 68 (2013) 713-720.

[22] P. Höppe, Different aspects of assessing indoor and outdoor thermal comfort, Energy and Buildings 34(6) (2002) 661-665.

[23] G. Katavoutas, H.A. Flocas, A. Matzarakis, Dynamic modeling of human thermal comfort after the transition from an indoor to an outdoor hot environment, International Journal of Biometeorology 59(2) (2015) 205-216.

[24] A.P. Gagge, A.P. Fobelets, L.G. Berglund, A standard predictive index of human response to the thermal environment, ASHRAE Transactions 92(1986) 709–731.

[25] J. Pickup, R. de Dear. An outdoor thermal comfort index (OUT_SET*), Part I: The model and its assumptions, Biometeorology and urban climatology at the turn of the millennium. Selected Papers from the Conference ICB-ICUC, 2000.

[26] H. Zhang, E. Arens, C. Huizenga, T, Han, Thermal sensation and comfort models for non-uniform and transient environments: Part I: Local sensation of individual body parts, Building and Environment 45(2) (2010) 380-388.

[27] D. Fiala, Dynamic Simulation of Human Heat Transfer and Thermal Comfort (PhD thesis), Leicester, UK: IESD, De Montfort University, 1998.

[28] R.V. Hogg, E. Tanis, D. Zimmerman, D, Probability and Statistical Inference, Pearson, London, 2014.

[29] ASHRAE, ASHRAE Handbook (SI), Fundamentals, 2009, American Society of Heating, Refrigerating and Air-conditioning Engineers, Inc., Atlanta, 2009.

[30] D. Lai, Q. Chen, A two-dimensional model for calculating heat transfer in the human body in a transient and non-uniform thermal environment, Energy and Buildings 118 (2016) 114-122.

[31] S. Dowdy, S. Wearden, D. Chilko, Statistics for Research. 3rd edition, A John Wiley and Sons, Inc. Publication, New Jersey, 2004.

[32] R Development Core Team, R: A Language and Environment for Statistical Computing, R Foundation for Statistical Computing, Vienna, Austria, 2008.

[33] H. Hensel, Thermal Sensation and Thermoreceptors in Man, Charles C Thomas Publisher, Springfield, 1982.

[34] R. de Dear, Revisiting an old hypothesis of human thermal perception: Alliesthesia, Building Research and Information 39(2) (2011) 108-117.

[35] R. Ferraro, S. Lillioja, A.M. Fontvieille, R. Rising, C. Bogardus, E. Ravussin, Lower sedentary metabolic rate in women compared with men, Journal of Clinical Investigation 90(3) (1992) 780-784.

[36] W. Schofield, Predicting basal metabolic rate, new standards and review of previous work, Human Nutrition Clinical Nutrition 39 (1984) 5-41.

[37] M. Kottek, J. Grieser, C. Beck, B. Rudolf, F. Rubel, World map of the Koppen-Geiger climate classification updated, Meteorologische Zeitschrift 15 (2006) 259-264.